Alleva et al., https://doi.org/10.1083/jcb.201606126

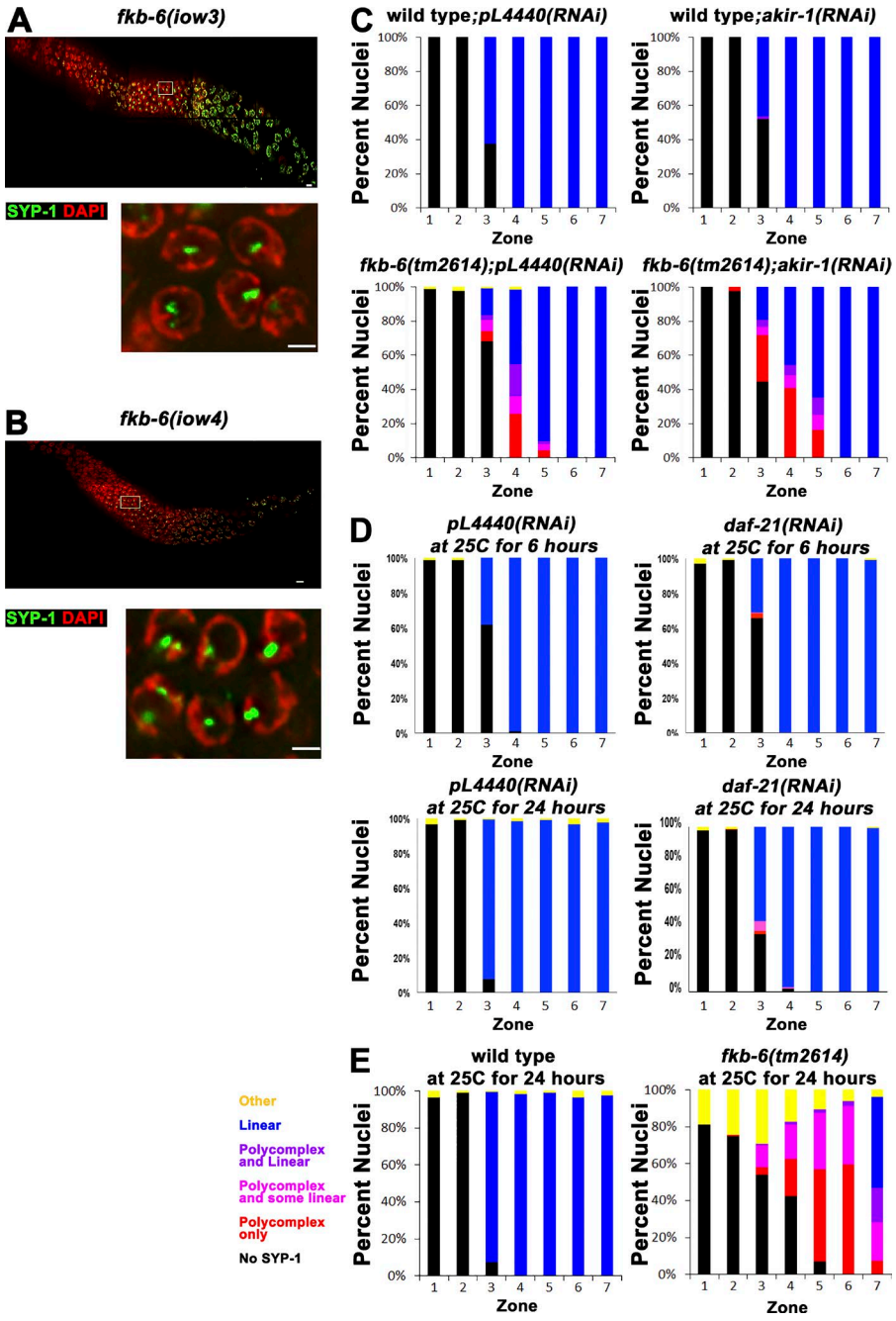

Figure S1. **Aggregation of SYP-1 proteins in *fkb-6(iow3)*, *fkb-6(iow4)*, *fkb-6(tm2614)*, *akir-1(RNAi)*, *daf-21*, and *fkb-6(tm2614)* mutants exposed to high temperature.** (A, top) *fkb-6(iow3)* mutant: images of full-length gonad stained with SYP-1 (central regions, red) and DAPI (blue). Image is a *z*-stack projection of half the germline. Bottom, projections of a *z*-stack halfway through the nuclei of the region boxed on the top. (B, top) *fkb-6(iow4)* mutant: images of full-length gonad stained with SYP-1 (central region SC, red) and DAPI (blue). Image is a *z*-stack projection of half the germline. Bottom, projections of a *z*-stack halfway through the nuclei of the region boxed on the top. Bars: (top) 5 µm; (bottom) 2 µm. (C) Quantification of SYP-1 staining of each of the indicated genotypes. Scoring was divided into six categories, as indicated in the panel. Representation of zones in terms of meiotic stage are as indicated in Fig. 1 D. *n* nuclei: *wild type;pl4440(RNAi)* = 834, *wild type;akir-1(RNAi)* = 958, *fkb-6;pl4440(RNAi)* = 899, and *fkb-6;akir-1(RNAi)* = 989. (D) RNAi of daf-21 does not result in PC formation. *daf-21(RNAi)* 6 h = 1,450, and *daf-21(RNAi)* 24 h = 1,277. (E) Exposing *fkb-6(tm2614)* mutants to high temperature increases PC formation. wild type = 1,339 and *fkb-6(tm2614)* = 742.

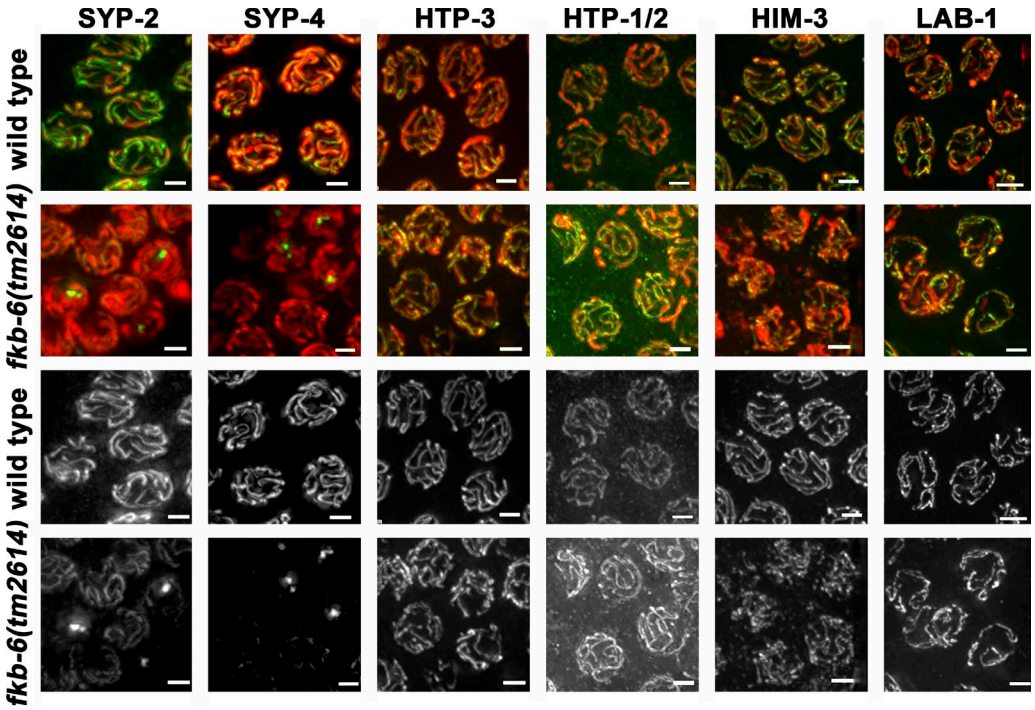

Figure S2. **Central region SC protein but not axial associated protein localization is affected in *fkb-6(tm2614)* mutants.** Representative images of MP in wild-type and *fkb-6(tm2614)* mutants stained with the indicated antibodies (labeled above each image, green) and DAPI (red; top two rows). Antibody stained only channel of the top row images also shown in white (bottom two rows). Images are *z*-stack projections halfway through the nuclei. Bars, 2 µm.

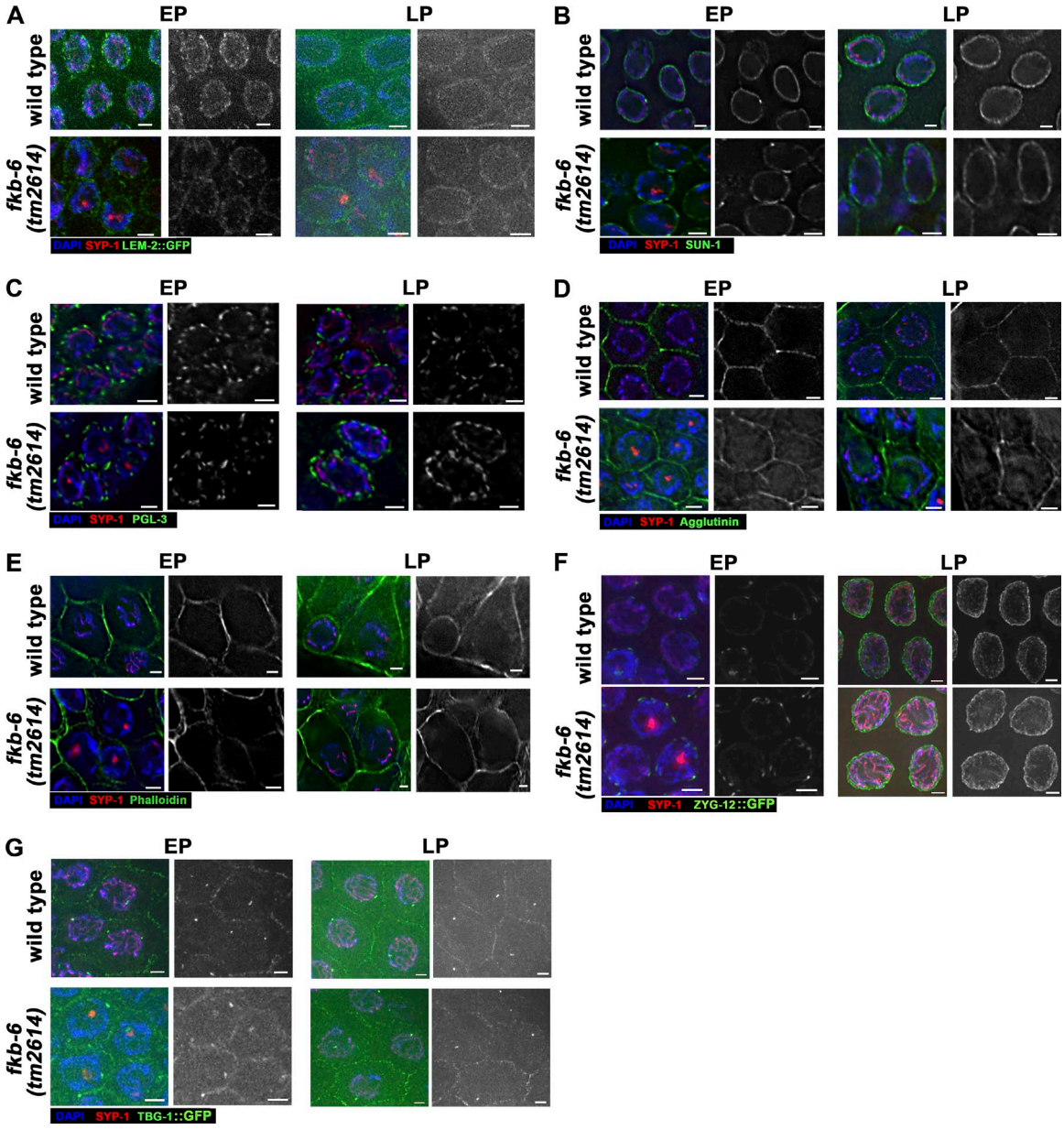

Figure S3. ***fkb-6(tm2614)* mutants have no defects in the localization of proteins found in the nuclear envelope, membrane, or F-actin.** (A) Representative images of GFP::LEM-2 localization in EP: SYP-1 (red), LEM-2 (green), and DAPI (blue). (B) Representative images of SUN-1 localization: SYP-1 (red), SUN-1 (green), and DAPI (blue). (C) Representative images of PGL-3 localization: SYP-1 (red), PGL-3 (green), and DAPI (blue). (D) Representative images of cell membrane (agglutinin staining): SYP-1 (red), agglutinin (green), and DAPI (blue). (E) Representative images of F-actin (phalloidin) localization: phalloidin (green), SYP-1 (red), and DAPI (blue). (F) Representative images of ZYG-12 localization: ZYG-12 (green), SYP-1 (red), and DAPI (blue). (G) Representative images of γ-tubulin localization: TBG-1 (green), SYP-1 (red), and DAPI (blue). All black-and-white panels have the green channel to left. All images show localization in wild-type and *fkb-6(tm2614)* mutants from EP and LP. All images are *z*-stacks of six 0.2-μm slices at the center of each nucleus. Bars, 2 μm.

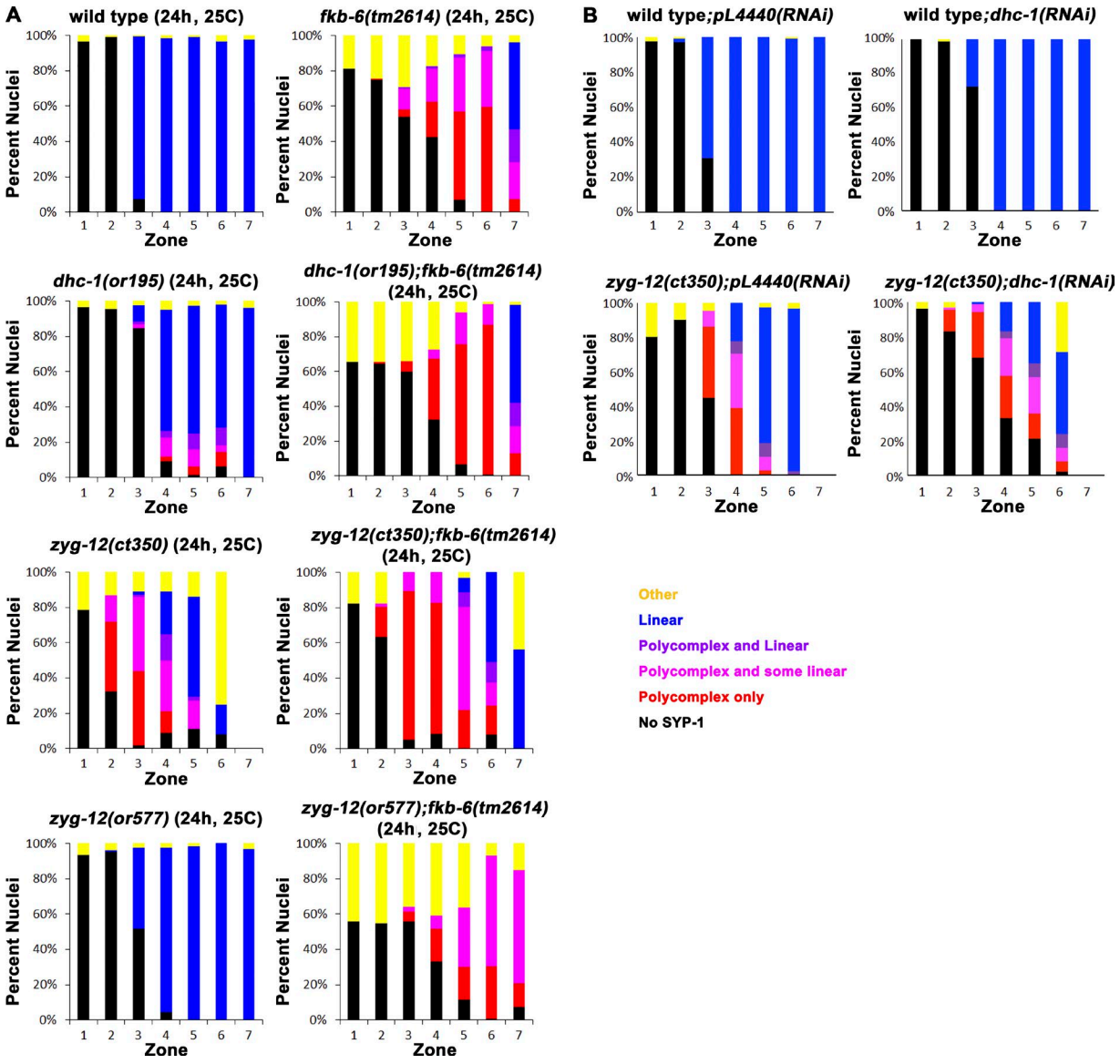

Figure S4. **Interactions between components regulating/required for chromosomal movement in PC formation.** (A) Quantification of SYP-1 staining of the indicated genotypes grown at 25°C for 24 h. *n* nuclei: wild type = 1,339, *fkb-6* = 742, *dhc-1* = 1,377, *fkb-6;dhc-1* = 795, *zyg-12(ct350)* = 398, *fkb-6;zyg-12(ct350)* = 316, *zyg-12(or577)* = 1,242, and *fkb-6;zyg-12(or577)* = 916. First two graphs are the same as in Fig. S1 E. (B) Quantification of SYP-1 staining of the indicated genotypes. *n* nuclei: wild type = 1,551, *dhc-1* = 1,749, *zyg-12(ct350)* = 398, *zyg-12(ct350);dhc-1(RNAi)* = 1,140, *zyg-12(or577)* = 496, and *fkb-6;zyg-12(or577)* = 789. Scoring was divided into six categories, as indicated in the panels. Representation of zones in terms of meiotic stage are as indicated in Fig. 1 E.

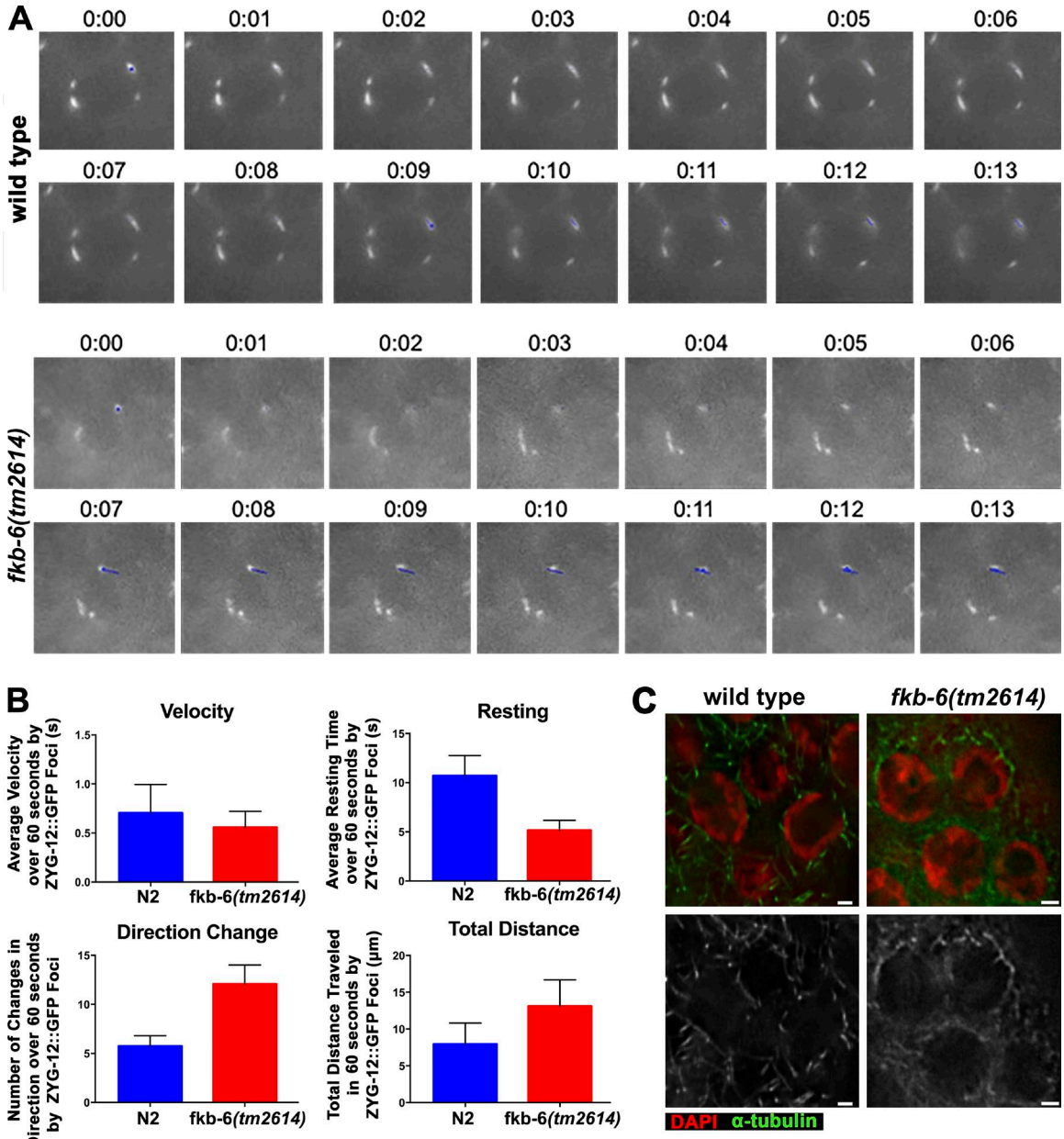

Figure S5. **Example of quantification of movement data, ZYG-12 movement, and microtubule organization.** (A) Time-lapse of DHC-1::GFP foci in N2 (top two rows) and *fkb-6(tm2614)* mutant (bottom two rows) backgrounds. Each blue dot represents a stopping point in DHC-1 focus movement. The blue line depicts the path of movement taken by the DHC-1 focus. Wild-type movement starts at time 0:00, ends at 0:09, and remains at rest until the end of the time-lapse. *fkb-6* mutant movement starts at time 0:00 and stops at times 0:07, 0:11, and 0:12. (B) Mean velocity, resting, change in direction, and total distance traveled by ZYG-12 patches in wild-type and *fkb-6(tm2614)* mutants. Error bars are SD. (C) Microtubule organization is altered next to the nuclear envelope in *fkb-6(tm2614)* mutants, α-tubulin (green) and DAPI (red). Images are a *z*-stack projection of a central section of the nuclei. Bars, 2 µm.

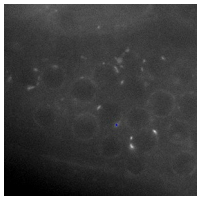

Video 1. **DHC-1::GFP live imaging in wild-type background.** Live imaging was done at the earliest (most distal) zone in which DHC-1::GFP foci are observed in pachytene of wild-type animals. The video is 4 s in length, representing eight images taken in total (image every 0.5 s). The white channel represents DHC-1::GFP. The blue line follows a singular DHC-1::GFP focus. Data from analyzed videos are presented in Fig. 6 (B–E).

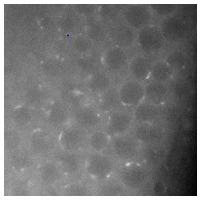

Video 2. **DHC-1::GFP live imaging in *fkb-6* mutant background.** Live imaging was done at the earliest (most distal) zone in which DHC-1::GFP foci are observed in pachytene of *fkb-6(tm2614)* mutant animals. The video is 4 s in length, representing eight images taken in total (image every 0.5 s). The white channel represents DHC-1::GFP. The blue line follows a singular DHC-1::GFP focus. Data from analyzed videos are presented in Fig. 6 (B–E).

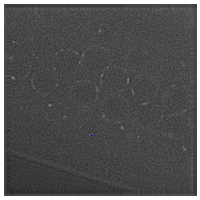

Video 3. **DHC-1::GFP live imaging in *syp-1* mutant background.** Live imaging was done at the earliest (most distal) zone in which DHC-1::GFP foci are observed in pachytene *syp-1(me17)* mutant animals. The video is 4 s in length, representing eight images taken in total (image every 0.5 s). The white channel represents DHC-1::GFP. The blue line follows a singular DHC-1::GFP focus. Data from analyzed videos is presented in Fig. 6 (B–E).